7466 *Inorg. Chem.* **2009**, *48*, 7466–7475
DOI: 10.1021/ic9006247

Inorganic Chemistry
Article

Thermodynamic and Kinetic Studies on Reactions of Fe^{III}(*meso*-[tetra-(3-sulfonatomesityl)porphin]) with NO in an Ionic Liquid. Trace Impurities Can Change the Mechanism!

Matthias Schmeisser and Rudi van Eldik*

Inorganic Chemistry, Department of Chemistry and Pharmacy, University of Erlangen-Nürnberg, Egerlandstrasse 1, 91058 Erlangen, Germany

Received March 31, 2009

To elucidate the applicability and effects of ionic liquids as reaction media for bioinorganic catalysis, detailed kinetic and mechanistic studies on the reversible binding of NO to the monohydroxo ligated iron(III) phorphyrin, (TMPS)Fe^{III}(OH) were performed in the ionic liquid [emim][NTf_2] as solvent. We report for the first time the determination of activation volumes via high pressure stopped flow methods in an ionic liquid. The studies clearly show that impurities of methylimidazole, present at the micromolar concentration level, can generate the 6-fold coordinated (TMPS)Fe^{III}(OH)-(MeIm) complex and lead to a complete changeover in mechanism from associatively activated for (TMPS)Fe^{III}(OH) to dissociatively activated for (TMPS)Fe^{III}(OH)(MeIm). NMR measurements on the chemical shift of the β-pyrrole protons revealed a spin state change from high spin ($S = 5/2$ for (TMPS)Fe^{III}(OH)) to an intermediate spin-state (S=5/2 and 3/2) following the coordination of methylimidazole. Because of the effect of the cationic component of the ionic liquid, Fe^{III}(TMPS) also reacts with nitrite unlike the case in aqueous solution. Kinetic and thermodynamic studies on the reaction of (TMPS)Fe^{III}(OH) with tetrabutylammonium nitrite allowed the determination of the equilibrium constant and thermodynamic parameters for the coordination of nitrite in [emim][NTf_2].

Introduction

During the past decade ionic liquids have received growing attention as alternative solvents for various applications. Because of their different tunable properties such as density, viscosity, polarity, melting point, and solubility, they enable the use of perfectly adapted reaction media and are even considered to be "designer solvents" of the future.[1−5] Although the use of some ionic liquids has already been well established in new technologies,[6,7] there is obviously still a lack of understanding of how these solvents actually influence or interact with substrates since some groups have reported an increase/decrease in reactivity or even a complete inhibition of reactions.[8,9] Therefore, we developed a general interest to quantify possible mechanistic changes and the reasons there for when a typical reaction of a catalytic active transition metal complex, extensively studied in conventional solvents before, is transferred into an ionic liquid. We recently reported on the significant effects of a series of ionic liquids, consisting of different anionic components, on substitution reactions of Pt^{II} complexes.[10]

Ionic liquids show a high solubility for several gases, especially for polar gases like CO_2, as a result of their specific inner structure with empty cavities between the cationic and anionic components. More systematic investigations indicate that gas solubility is on the one hand an effect of the polarity and polarizability of a gas, and on the other hand depends on the nature and steric features of the cationic and anionic components. Thus, tailor-made ionic liquids are also considered as storage media for harmful gases or as a separation agent for gas mixtures.[11−14]

*To whom correspondence should be addressed. E-mail: vaneldik@chemie.uni-erlangen.de.

(1) Wasserscheid, P. *Chemie in unserer Zeit* **2003**, *1*, 52–63.
(2) Wasserscheid, P.; Keim, W. *Angew. Chem.* **2000**, *112*, 3926–3945.
(3) Luo, S.; Mi, X.; Zhang, L.; Lui, S.; Xu, H.; Cheng, J. P. *Angew. Chem., Int. Ed.* **2006**, *45*, 3093–3097.
(4) Freemantle, M. *Chem. Eng. News* **1998**, *76*, 32–37.
(5) Davis, J. H. *Chem. Lett.* **2004**, *33*, 1072–1077.
(6) Maase, M. *Multiphase Homogeneous Catal.* **2005**, *2*, 560–566.
(7) Tempel, D.; Henderson, P.; Brzozowski, J.; Pearlstein, R.; Garg, D. U. S. Patent Application Publ. **2006**, 15 pp Cont.-in-part of U.S. Ser. No. 9482, 277.
(8) Mc. Nulty, J.; Cheekoori, S.; Bender, T. P.; Coggan, J. A. *Eur. J. Org. Chem.* **2007**, *9*, 1423–1428.
(9) Daguenet, C.; Dyson, P. *Organometallics* **2006**, *25*, 5811–5816.
(10) (a) Begel, S.; Illner, P.; Kern, S.; Puchta, R.; van Eldik, R. *Inorg. Chem.* **2008**, *47*, 7121–7132. (b) Illner, P.; Begel, S.; Kern, S.; Puchta, R.; van Eldik, R. *Inorg. Chem.* **2009**, *48*, 588–597.
(11) Bremse, J.; Alejandre, J. *J. Chem. Phys.* **2003**, *118*, 4134–4139.
(12) (a) Anderson, J. L.; Dixon, J. K.; Brennecke, J. *Acc. Chem. Res.* **2007**, *40*, 1208–1216. (b) Anthony, J. L.; Maginn, E. J.; Brennecke, J. *J. Phys. Chem. B* **2002**, *106*, 7315–7320.
(13) Camper, D.; Scovazzo, P.; Koval, C.; Noble, R. *Ind. Eng. Chem. Res.* **2004**, *43*, 3049–3054.
(14) Anthony, J. L.; Anderson, J. L.; Maginn, E. J.; Brennecke, J. *J. Phys. Chem. B* **2005**, *109*, 6366–6374.

Published on Web 06/18/2009

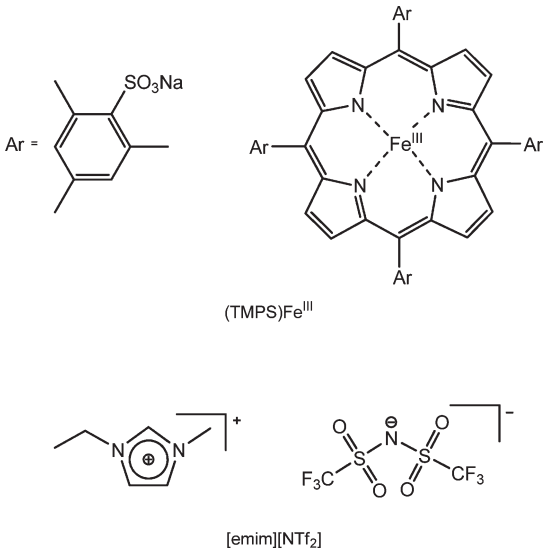

Figure 1. Structures of (TMPS)Fe^{III} and [emim][NTf_2].

Ferriheme proteins play an important role in mammalian biology; they trigger, accompany, and catalyze numerous physiological reactions. The transport of oxygen by erythrocytes, the deactivation of peroxide by Cytochrome c, or the activation of soluble Guanylylcyclase (sGC) by nitric oxide as an instrument to regulate the blood pressure are only a few examples of the high versatility of these enzymes.[15−18] Over the past years our group extensively studied the reaction between different modified, water-soluble Fe^{III}(porphyrin) complexes and dissolved nitric oxide gas as model systems for ferriheme proteins to elucidate their nature and mechanistic behavior in vivo.[19,20]

It is now our aim to investigate the influence of ionic liquids as new designer solvents on the catalytic activity of model bioinorganic systems. For our first study we selected the reaction between *meso*-[tetra(3-sulfonatomesityl)porphin]-iron(III), Fe^{III}(TMPS), and dissolved nitric oxide (NO) in the ionic liquid 1-ethyl-3-methylimidazolium bis-trifluoromethylsulfonylamide, [emim][NTf_2], as reaction medium (see Figure 1). We expected this liquid to be well suited because of its low viscosity (34 cP at 20 °C), hydrophobic nature, and optical purity in the spectral region of typical porphyrin absorbances (300−800 nm). Earlier studies in aqueous solution clearly showed that Fe^{III}(TMPS) exists, depending on the pH, as 6-fold coordinated diaqua ((TMPS)Fe^{III}-$(H_2O)_2$), or as 5-fold coordinated monohydroxo ((TMPS)-Fe^{III}(OH)) species ($pK_a = 6.9$). Although the binding of NO to the monohydroxo species exhibits an associative mechanism, the 6-fold coordinated diaqua species on the contrary reacts much faster. This observation is ascribed to a smaller overall spin state change of the porphyrin iron(III) center that occurs on the binding of NO to the diaqua species. Therefore, in aqueous solution NO coordination is not controlled by the lability/accessibility of the iron(III) center but rather by the Fe-NO bond formation step.[21−23] We checked the reaction behavior in ionic liquid by performing kinetic studies using stopped-flow techniques at ambient and high pressure. During our work we surprisingly found that despite its negatively charged sulfonato substituents, Fe^{III}(TMPS) in ionic liquid reacts not only with nitric oxide but also with nitrite either as an added reactant or as impurity in solutions of NO. Therefore, we extended our studies to the reaction of Fe^{III}(TMPS) with terabutylammoniumnitrite and also determined its kinetic and thermodynamic parameters.

Experimental Section

Materials. All chemicals used were of analytical reagent grade or of the highest purity commercially available. The iron porphyrin, [*meso*-tetra(3-sulfonatomesityl)porphine]-iron(III) hydroxide (tetrasodium salt), was purchased from Frontier Scientific Ltd., Utah, U.S.A. and used without further purification. NO gas (Praxair Deutschland GmbH & Co. KG, Bopfingen, purity 3.0) was cleansed from trace amounts of higher nitrogen oxides by passing it through concentrated KOH solution, an Ascarite II column (NaOH, on silica gel, Sigma-Aldrich), and a phosphorus pentoxide column. Tetrabutylammoniumnitrite (Sigma-Aldrich) was stored under argon atmosphere.

Synthesis of the Ionic Liquid. All operations were performed under nitrogen atmosphere. [emim]Br and Li[NTf_2] were purchased from Solvent Innovation or Iolitec, and [emim]Br was purified twice by recrystallization (methanol/acetone 1:10) and obtained as white solid. [emim][NTf_2] was synthesized according to an anion metathesis procedure described in the literature.[24] The synthesized [emim][NTf_2] was treated with activated charcoal, dried under vacuum, and obtained as colorless liquid. The water content of the ionic liquid, determined by Karl Fisher titration,[25] was found to be 40−70 ppm.

Instrumentation. Karl Fischer titrations were done on a 756 KF Coulometer. Elemental analyses (Euro EA 3000 (Euro vector) and EA 1108 (CarloErba)) and NMR spectroscopy (Bruker Avance DRX 400WB FT-spectrometer) were used for chemical analysis. UV−vis spectra were recorded in gastight cuvettes on a Varian Cary 1G spectrophotometer equipped with a thermostatted cell holder.

Stopped-Flow Studies with NO. Stopped-flow kinetic measurements at ambient pressure were performed on a Durrum D110 (Dionex) stopped-flow instrument. In a typical experiment, deoxygenated [emim][NTf_2] was mixed in varying volume ratios with a saturated NO solution in gastight syringes to obtain the appropriate NO concentration (1−10 mM).[26,27] The NO solution was then rapidly mixed with a deoxygenated solution of the Fe^{III}(TMPS) (5−6 μM) in a 1:1 volume ratio in the stopped-flow apparatus. The kinetics of the reaction were monitored at 434 nm. All kinetic experiments were performed under pseudo-first-order conditions, that is, with at least a 10-fold excess of NO over Fe^{III}(TMPS). Rate constants reported are mean values of at least five kinetic runs, and the quoted uncertainties are based on standard deviations. High pressure stopped-flow experiments were performed at pressures up to 130 MPa on a custom-built

(15) Rand, M. J.; Li, C. G. *Annu. Rev. Physiol.* **1995**, *38*, 659–682.
(16) Pfeiffer, S.; Mayer, B.; Hemmens, B. *Angew. Chem., Int. Ed.* **1999**, *38*, 1714–1731.
(17) Ignarro, L. J. *Angew. Chem., Int. Ed.* **1999**, *38*, 1882–1892.
(18) Denisov, L. G.; Makris, T. M.; Sligar, S. G.; Schlichting, I. *Chem. Rev.* **2005**, *105*, 2253–2277.
(19) Franke, A.; Roncaroli, F.; van Eldik, R. *Eur. J. Inorg. Chem.* **2007**, *6*, 773–798.
(20) van Eldik, R. *Coord. Chem. Rev.* **2007**, *251*, 1649–1662.
(21) Laverman, L. E.; Hoshino, M.; Ford, P. C. *J. Am. Chem. Soc.* **1997**, *119*, 12663–12664.
(22) Laverman, L. E.; Ford, P. C. *J. Am. Chem. Soc.* **2001**, *123*, 11614–11622.
(23) Wolak, M.; van Eldik, R. *J. Am. Chem. Soc.* **2005**, *127*, 13312–13315.
(24) Bonhôte, P.; Dias, A. P.; Papageorgiou, N.; Kalyanasundaram, K.; Grätzel, M. *Inorg. Chem.* **1996**, *35*, 1168–1178.
(25) Schöffski, K. *Chemie in unserer Zeit* **2000**, *34*, 170–175.
(26) Unpublished results; for the general procedure used to determine the solubility of NO see reference 27.
(27) Wasserscheid, P. *Ionic liquids in synthesis*; Welton, T., Ed.; Wiley-VCH: Weinheim, Germany, 2003; p 81.

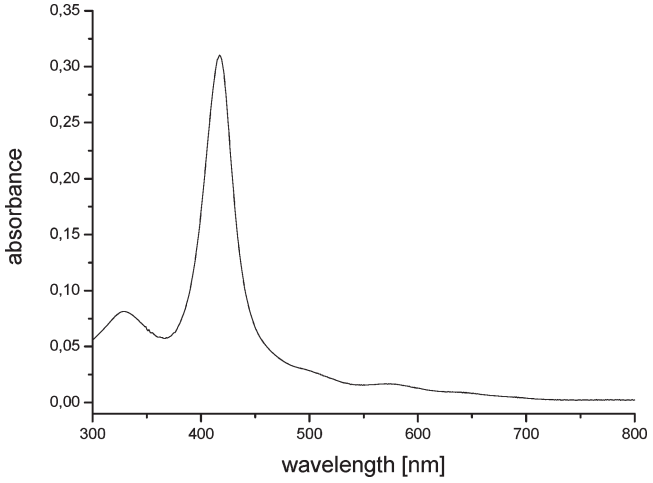

Figure 2. UV−vis spectrum of (TMPS)Fe^{III} in [emim][NTf_2]. Experimental conditions: [Fe^{III}(TMPS)] = 3×10^{-6} M, optical path length 1 cm.

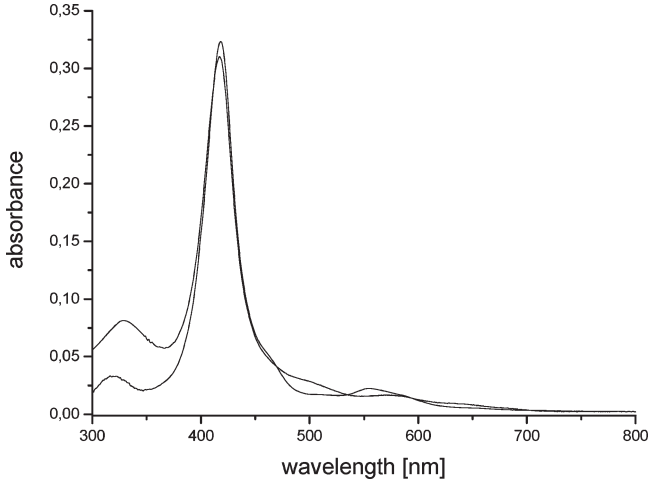

Figure 3. Comparative UV−vis spectra for both observed species of Fe^{III}(TMPS) in [emim][NTf_2]. Experimental conditions: [Fe^{III}(TMPS)] = 3×10^{-6} M, optical path length 1 cm.

instrument with heptane as pressure medium as described elsewhere.[28] Kinetic traces were analyzed with the use of Origin 7G SR4 (Originlab Corporation) software.

Stopped-Flow Studies with NO_2^-. Solutions containing nitrite were prepared by dissolving tetrabutylammoniumnitrite in [emim][NTf_2]. Sodium- or potassium-nitrite seemed not to be soluble in [emim][NTf_2]. Concentrations were adjusted up to 300-fold excess of NO_2^- over Fe^{III}(TMPS). The kinetics of the reaction were monitored at 424 nm. The measurements were performed and analyzed as described above for NO. The equilibrium constant (K_{eq}) was determined from the slope and intercept of a linear plot of k_{obs} versus [NO_2^-] as described in Results and Discussion.

Thermodynamic Studies on the Reaction with Nitrite. Solutions were prepared as mentioned above. The equilibrium constant K_{eq} was determined via absorbance change measurements at 424 nm in tandem cuvette experiments with concentrations up to 1000-fold excess of NO_2^- over (TMPS)Fe^{III}. The pressure dependence of the equilibrium constant (K_{eq}) was measured at pressures up to 150 MPa on a Shimadzu UV-2101 PC UV−vis spectrophotometer equipped with a custom-built high pressure cell and the use of a quartz pill-box cuvette.[29]

Results and Discussion

Preliminary Observations on Fe^{III}(TMPS) in [emim][NTf_2]. To establish the nature of the iron porphyrin species present in [emim][NTf_2], UV−vis experiments clearly show a maximum of the Soret band at 417 nm (Figure 2), which indicates the presence of a monohydroxo-coordinated iron(III) species (TMPS)Fe^{III}-(OH) as found in water under basic conditions.[23] The spectral features observed are in good agreement with those reported for other monohydroxo-coordinated iron (III) porphyrins in organic[30] and aqueous solvents.[31]

Attempts to generate the six-coordinate diaqua species, (TMPS)$Fe^{III}(H_2O)_2$, by successive addition of *p*-toluenesulfonic acid only led to the protonation of the pyrrolic nitrogen atoms and therefore to demetalation of the porphyrin. Thus, in [emim][NTf_2] the monohydroxo species (TMPS)Fe^{III}(OH) seems to be the only stable complex.

Depending on the batch of ionic liquid used, we observed large kinetic and mechanistic differences for the binding of NO to the Fe^{III}(TMPS) complex, which indicated a pre-occupation of the sixth coordination site at the porphyrin iron(III) center in some cases. Our first assumption that this coordination is caused by the "innocent" [NTf_2] anion[32] could not be confirmed by spin state measurements on the iron(III) center. ^{1}H NMR spectroscopy is a widely recognized method to characterize the spin and ligation states of paramagnetic iron porphyrins. In particular, the chemical shift of the β-pyrrole protons in iron(III) porphyrins has proven to be an excellent probe to determine the spin state of the iron(III) center.[33] However, ^{1}H NMR experiments performed in aqueous solution did not result in a shift of the β-pyrrole protons after the addition of even large amounts of Li[NTf_2]. A closer look at the UV−vis spectra, especially at the Q-band pattern, clearly showed the formation of two different species of the (TMPS)Fe^{III}(OH) complex, which unequivocally differed in absorbances at 325, 500, 550, and 650 nm as can be seen in Figure 3. The Soret band on the contrary is only slightly influenced and shows a red-shift of 1 nm to 418 nm.

HPLC studies on the purity of strange reacting batches of the ionic liquid verified a contamination by small amounts of methylimidazole, MeIm (for experimental conditions see Figure S1, Supporting Information), which is used as starting material in the synthesis of

(28) (a) van Eldik, R.; Palmer, D. A.; Schmidt, R.; Kelm, H. *Inorg. Chim. Acta* **1981**, *50*, 131–135. (b) van Eldik, R.; Gaede, W.; Wieland, S.; Kraft, J.; Spitzer, M.; Palmer, D. A. *Rev. Sci. Instrum.* **1993**, *64*, 1355–1357.

(29) Spitzer, M.; Gärtig, F.; van Eldik, R. *Rev. Sci. Instrum.* **1988**, *59*, 2092–1093.

(30) (a) Woon, T. C.; Shirazi, A.; Bruice, T. *Inorg. Chem.* **1986**, *25*, 3845–3846. (b) Cheng, R. J.; Latos-Grazynski, L.; Balch, A. *Inorg. Chem.* **1982**, *21*, 2412–2418.

(31) (a) Zipplies, M. F.; Lee, W. A.; Bruice, T. C. *J. Am. Chem. Soc.* **1986**, *108*, 4433–4435. (b) Tondreau, G. A.; Wilkins, R. G. *Inorg. Chem.* **1986**, *25*, 2745–2750. (c) El-Awady, A. A.; Wilkins, P. C.; Wilkins, R. G. *Inorg. Chem.* **1985**, *24*, 2053–2073.

(32) (a) Mudring, A.-V.; Babai, A.; Arenz, S.; Giernoth, R. *Angew. Chem., Int. Ed.* **2005**, *44*, 5485–5488. (b) Williams, D. B.; Stoll, M. E.; Scott, B. L.; Costa, D. A.; Oldham, W. J. *Chem. Commun.* **2005**, 1438–1440.

(33) (a) Walker, F. A. In *The Porphyrin Handbook*; Kadish, K. M., Smith, K. M., Guilard, R., Eds.; Academic Press: San Diego, CA, 2000; Vol 5, Chapter 36, pp 81−183. (b) Ivanca, M. A.; Lappin, A. G.; Scheidt, W. R. Inorg. Chem. 1991, 30, 711–718.

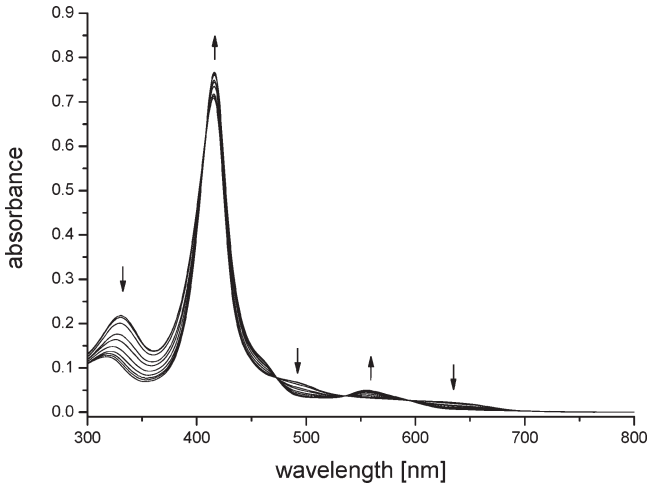

Figure 4. UV−vis spectral changes after subsequent addition of an up to 200 fold excess of methylimidazole over (TMPS)Fe^{III} (OH) in aqueous solution at pH 8.3. Experimental conditions: [(TMPS)Fe^{III}(OH)] = 7.5×10^{-6} M, [Tris buffer] = 0.07 M (adjusted with $HClO_4$).

[emim]Br.[24] Unfortunately, we were not able to remove this impurity completely, despite 2-fold recrystallization of [emim]Br and further purification of the resulting ionic liquid [emim][NTf_2] with activated charcoal. Calculations based on the recorded HPLC-chromatogram quantified the contamination to be about 6 μM.[34] As can be seen from Figure 4, the addition of MeIm up to a 200 fold excess over (TMPS)Fe^{III}(OH) in an aqueous buffer solution leads to the same spectral changes as observed in Figure 3. Clean isosbestic points at 407, 474, 535, and 595 nm confirm the direct generation of a six-coordinate (TMPS)Fe^{III}(OH)(MeIm) species (see also section on the binding of NO to (TMPS)Fe^{III}(OH)(MeIm)) with a different reaction behavior than the five-coordinate (TMPS)Fe^{III}(OH) complex). The results for both species are now presented and discussed separately.

Binding of NO to (TMPS)Fe^{III}(OH). The addition of NO gas to a deoxygenated solution of (TMPS)Fe^{III}(OH) resulted in spectral changes presented in Figure 5. The decrease in absorbance at 417 nm accompanied by the appearance of new bands at 434 and 548 nm indicates the formation of a typical low-spin iron(III) porphinato-nitrosyl complex[4,35] in which the formal charge distribution can be described as (TMPS)Fe^{II}(OH)(NO^+) because of its diamagnetic behavior. Bubbling of an inert gas through the resulting solution leads to reversed spectral changes indicating reversibility of reaction 1.

$$(\mathrm{TMPS})\mathrm{Fe^{III}(OH)} + \mathrm{NO} \underset{k_{off}}{\overset{k_{on}}{\rightleftarrows}} (\mathrm{TMPS})\mathrm{Fe^{II}(OH)(NO^+)} \quad (1)$$

The binding of NO is followed by a subsequent slow reaction on a time scale of several hours, leading to new maxima at 406 and 475 nm, with clean isosbestic points at 419, 446, and 539 nm. This reaction is ascribed to the formation of (TMPS)Fe^{II}(NO•) via hydroxide or nitrite

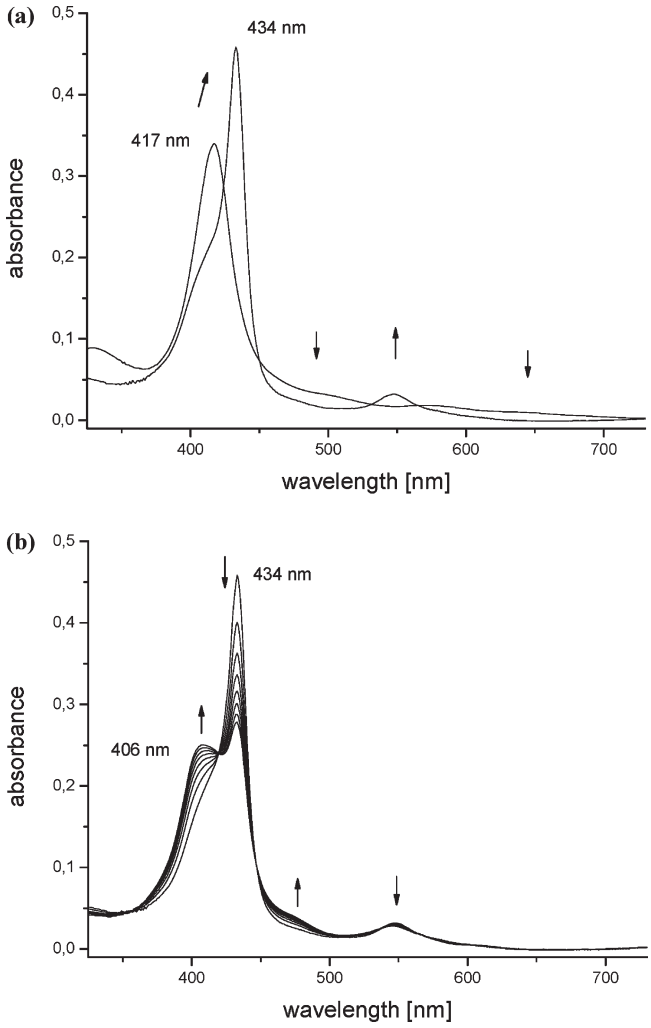

Figure 5. Spectral changes recorded after addition of NO gas to a solution of (TMPS)Fe^{III} (OH) in [emim][NTf_2]: (a) Binding of NO to (TMPS)Fe^{III} (OH); (b) Subsequent slow reductive nitrosylation. Experimental conditions: [(TMPS)Fe^{III}(OH)] = 3×10^{-6} M, optical path length 1 cm.

catalyzed reductive nitrosylation. Reduction of (TMPS)-Fe^{III}(OH) by use of ethanethiol and subsequent addition of NO resulted in the same final spectrum, that is, the formation of (TMPS)Fe^{II}(NO•).[36−38]

The kinetics of the reversible binding of NO to (TMPS)-Fe^{III}(OH) was investigated by stopped-flow technique under pseudo-first-order conditions with at least a 10-fold excess of NO. The k_{obs} values determined by fitting the kinetic traces to a single exponential function depend linearly on [NO] according to eq 2 based on the data in Figure 6.

$$k_{obs} = k_{on}[\mathrm{NO}] + k_{off} \quad (2)$$

The linear fit of k_{obs} versus [NO] obtained at 25 °C allowed the calculation of $k_{on} = (1.040 \pm 0.002) \times 10^2$ M^{-1} s^{-1} and $k_{off} = 0.030 \pm 0.007$ s^{-1} from the slope and intercept, respectively. The overall equilibrium

(34) Sola, J. L. C.; Koenig, A., in preparation.
(35) Theodoridis, A.; van Eldik, R. *J. Mol. Catal. A: Chem.* **2004**, *224*, 197–205.
(36) Jee, J.-E.; van Eldik, R. *Inorg. Chem.* **2006**, *45*, 6523–6534.
(37) Jee, J.-E.; Eigler, S.; Jux, N.; Zahl, A.; van Eldik, R. *Inorg. Chem.* **2007**, *46*, 3336–3352.
(38) Ford, P. C.; Fernandez, B. O.; Lim, M. D. *Chem. Rev.* **2005**, *105*, 2439–2455.

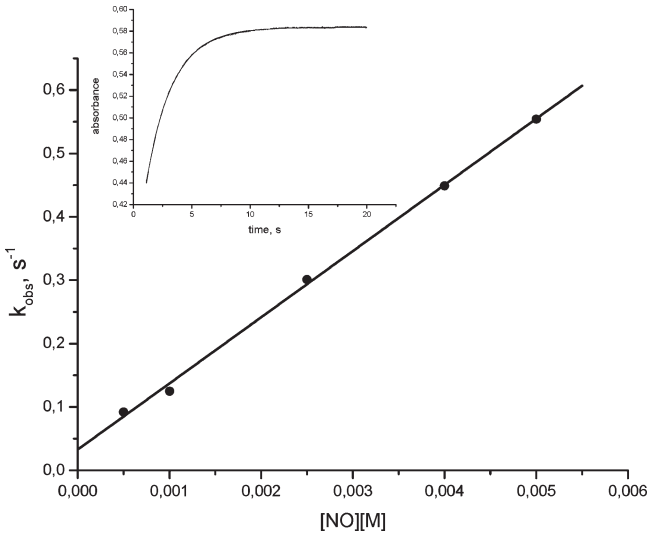

Figure 6. Concentration dependence of k_{obs} for the reaction of (TMPS)-Fe^{III}(OH) with NO in [emim][NTf_2]. Experimental conditions: [(TMPS)-Fe^{III}(OH)] = 3×10^{-6} M, λ = 434 nm, T = 25 °C. Inset: typical kinetic trace, [NO] = 5 mM.

constant was found to be $K_{NO} = k_{on}/k_{off} = (3.5 \pm 0.8) \times 10^3$ M^{-1}. To determine the activation parameters $\Delta H^{\ddagger}$, $\Delta S^{\ddagger}$, and $\Delta V^{\ddagger}$ for the binding of NO, the kinetics were studied at different temperatures (25−45 °C) and pressures (10−130 MPa) at the highest [NO] = 5 mM to minimize the contribution of the small intercept in the concentration dependence, that is, $k_{obs} = k_{on}$[NO] under these conditions. The Eyring plot for the temperature dependence and a plot of ln k_{obs} versus pressure are shown in Figure 7.

The activation parameters calculated from these plots are summarized in Table 1 and compared with the data found in basic aqueous solution.[23] The binding of NO is much slower in [emim][NTf_2] than in water, in agreement with a higher activation enthalpy ($\Delta H^{\ddagger}$) value. The increase in the activation barrier may be caused by the ionic strength and the polarity of the ionic liquid. We recently reported similar deceleration effects for ligand substitution reactions of Pt(II) complexes performed in various ionic liquids.[10] The significantly negative values for $\Delta S^{\ddagger}$ and $\Delta V^{\ddagger}$ suggest that the binding of NO to (TMPS)Fe^{III}(OH) occurs according to an associative (A) mechanism. From the activation parameters it follows that the sixth coordination site at the iron center seems to be unoccupied. The relatively large negative activation volume can be explained by a movement of the iron(III) center from out of the porphyrin plane into the porphyrin plane on the binding of NO, as shown in Scheme 1.[39] Unfortunately, NMR measurements on the spin state of the iron(III) center could not be performed directly in [emim][NTf_2] because of the low solubility of the porphyrin complex. However, the kinetic data, which are similar to the results found for aqueous solution, lead to the conclusion that the spin state of the iron(III) center is not, or only weakly, influenced by the ionic liquid. Thus, we ascribe the nature of (TMPS)Fe^{III}(OH) in

(39) Jee, J.-E.; Eigler, S.; Hampel F.; Jux, N.; Wolak, M.; Zahl, A.; Stochel, G.; van Eldik, R. *Inorg. Chem.* **2005**, *44*, 7717-7731, and references cited therein.

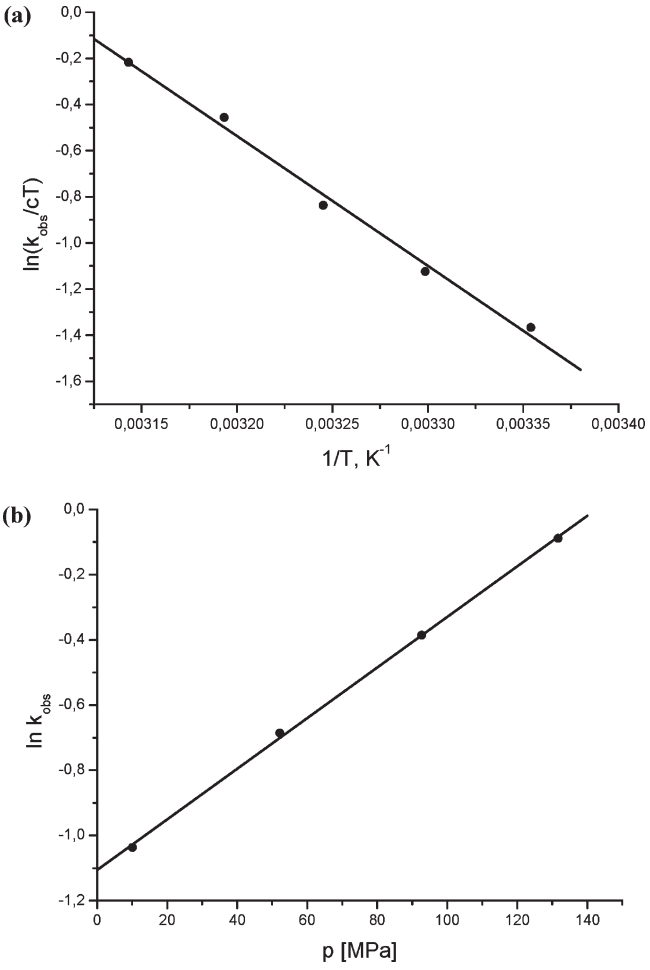

Figure 7. Temperature and pressure dependence for the binding of NO to (TMPS)Fe^{III}(OH) in [emim[NTf_2]. Experimental conditions: [(TMPS)-Fe^{III}(OH)] = 3×10^{-6} M, [NO] = 5 mM, λ = 434 nm.

Scheme 1. Spin State Change of the Porphyrin Iron Center after Binding of NO

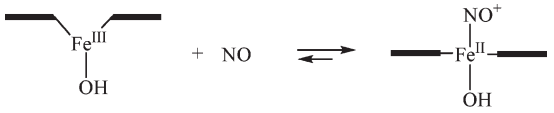

high spin low spin

[emim][NTf_2] as a high-spin iron(III) porphyrin which undergoes a spin-state change from a high-spin (S = 5/2) to a diamagnetic low-spin state (S = 0) on the reaction with NO.

Binding of NO to (TMPS)Fe^{III}(OH)(MeIm). The spectral changes that accompany the reaction of (TMPS)-Fe^{III}(OH)(MeIm) with NO lead to a final spectrum with the same characteristic bands at 434 and 548 nm as observed above for (TMPS)Fe^{II}(OH)(NO^+). Thus the binding of NO to (TMPS)Fe^{III}(OH)(MeIm) seems to generate the same product as found for (TMPS)Fe^{III}(OH) (Figure 8). This reaction also undergoes subsequent reductive nitrosylation as indicated by a weak shoulder at 406 nm.

The increase in absorbance followed at 434 nm occurred on a much longer time scale than observed for the binding of NO to (TMPS)Fe^{III}(OH). Kinetic measure-

Table 1. Rate Constants and Activation Parameters for the Binding of NO to (TMPS)Fe^{III} in [emim][NTf_2] and Aqueous Solution

	(TMPS)Fe^{III}-(OH) in [emim][NTf_2]	(TMPS)Fe^{III}-(OH)(MeIm) in [emim][NTf_2]	(TMPS)Fe^{III}-(OH) in water at pH 11
overall rate constant	$(1.040 \pm 0.002) \times 10^2$ M^{-1} s^{-1} (second order)	0.070 ± 0.002 s^{-1} (first order)	$(13.2 \pm 0.1) \times 10^3$ M^{-1} s^{-1} (second order)
$\Delta H^{\ddagger}$ (kJ mol^{-1})	47 ± 2	106 ± 7	28 ± 1
$\Delta S^{\ddagger}$ (J K^{-1} mol^{-1})	-53 ± 7	$+86 \pm 21$	-71 ± 2
$\Delta V^{\ddagger}$ (cm^3 mol^{-1})	-20 ± 1	$+24 \pm 1$	-16.2 ± 0.4

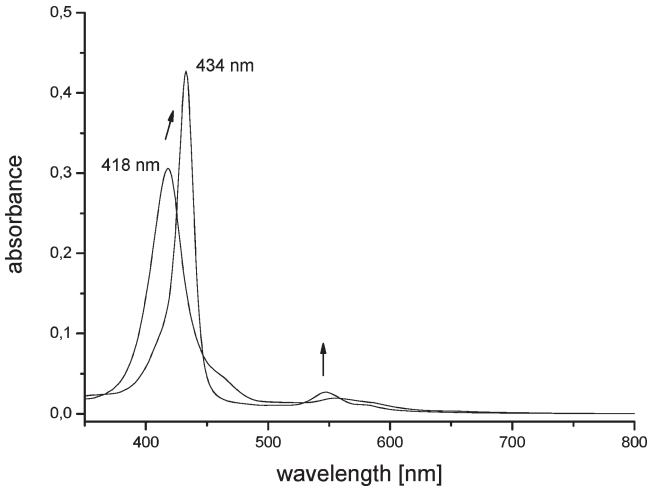

Figure 8. Spectral changes after addition of NO gas to a solution of (TMPS)Fe^{III}(OH)(MeIm) in [emim][NTf_2]. Experimental conditions: [(TMPS)Fe^{III}(OH)(MeIm)] = 2.5×10^{-6} M, optical path length 1 cm.

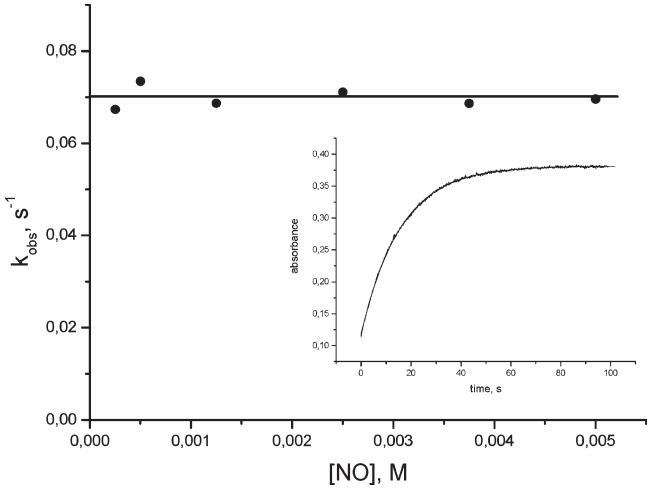

Figure 9. Concentration dependence of k_{obs} for the reaction of (TMPS)-Fe^{III}(OH)(MeIm) with NO in [emim][NTf_2]. Experimental conditions: [(TMPS)Fe^{III}(OH)(MeIm)] = 2.5×10^{-6} M, λ = 434 nm, T = 25 °C. Inset: typical kinetic trace, [NO] = 5 mM.

ments performed under pseudo-first-order conditions at 25 °C and fitted to a single exponential function surprisingly showed no dependence on [NO] (Figure 9). This suggests that the binding of NO to (TMPS)Fe^{III}(OH) (MeIm) follows a limiting dissociative (D) mechanism as outlined in eq 3.

$$\text{(TMPS)Fe}^{\text{III}}\text{(OH)(MeIm)} \underset{k_{-1}}{\overset{k_1}{\rightleftharpoons}} \text{(TMPS)Fe}^{\text{III}}\text{(OH)} + \text{MeIm}$$

$$\text{(TMPS)Fe}^{\text{III}}\text{(OH)} \xrightarrow[k_2]{+\text{NO}} \text{(TMPS)Fe}^{\text{II}}\text{(OH)(NO}^{+}\text{)} \qquad (3)$$

For this mechanism the observed rate constant k_{obs} is expressed as in eq 4, and the kinetic data are expected to show a saturation behavior on applying steady state conditions to (TMPS)Fe^{III}(OH).

$$k_{obs} = \frac{k_1 k_2 [\text{NO}]}{k_{-1}[\text{MeIm}] + k_2[\text{NO}]} \qquad (4)$$

If k_2[NO] $\gg$ k_{-1}[MeIm], that is, the reaction with NO is much faster than the back reaction with traces of MeIm, the expression for the observed rate constant in eq 4 reduces to eq 5 and shows no dependence on [NO].

$$k_{obs} = k_1 \qquad (5)$$

Thus the observed kinetic data imply that the dissociation of MeIm is the rate-limiting step under these experimental conditions and not the binding of NO. The average value of k_{obs} was calculated to be 0.070 ± 0.002 s^{-1} at 25 °C. Kinetic measurements at [NO] = 5 mM performed in the temperature range of 15−35 °C allowed the construction of an Eyring plot and the estimation of the activation parameters $\Delta H^{\ddagger} = 106 \pm 7$ kJ mol^{-1} and $\Delta S^{\ddagger} = +86 \pm 21$ J K^{-1} mol^{-1}. Especially the significant positive value of the activation entropy supports the dissociation of MeIm as the rate-limiting step with a high activation barrier and points to the strong binding of MeIm to (TMPS)Fe^{III}(OH). The activation volume, $\Delta V^{\ddagger} = +24 \pm 1$ cm^3 mol^{-1}, determined from a linear plot of ln k_1 versus pressure (see Figure 10), confirms the operation of a limiting dissociative (D) mechanism characterized by a voluminous transition state.

Altogether the coordination of MeIm to (TMPS)-Fe^{III}(OH) has a large influence on the kinetics and mechanistic behavior toward the binding of NO. In the case of a strong coordination of MeIm, the spin state of the iron(III) center should be influenced significantly. Earlier studies on (TMP)$Fe^{III}(ClO_4)$, TMP = [*meso*-tetra(2,4,6 trimethylphenyl)-porphine], in CH_2Cl_2 as solvent reported on the coordination of various modified imidazoles (also methylimidazole) and their effect on the spin state of the iron(III) center.[40] In our case ^{1}H NMR spectroscopy on the chemical shift of the β-pyrrole protons (for experimental conditions and NMR spectra see Figures S2 and S3, Supporting Information) showed the direct appearance of a signal at −16 ppm on the addition of deuterated imidazole (deuterated MeIm was not available).[41] This confirms the formation of a 6-fold

(40) Ikezaki, A.; Nakamura, M. *Inorg. Chem.* **2002**, *41*, 6225–6236.

(41) We observed the same UV−vis spectral changes for the coordination of imidazole to (TMPS)Fe^{III}(OH), thus NMR experiments performed on imidazole should lead to the same results as for MeIm (see Supporting Information).

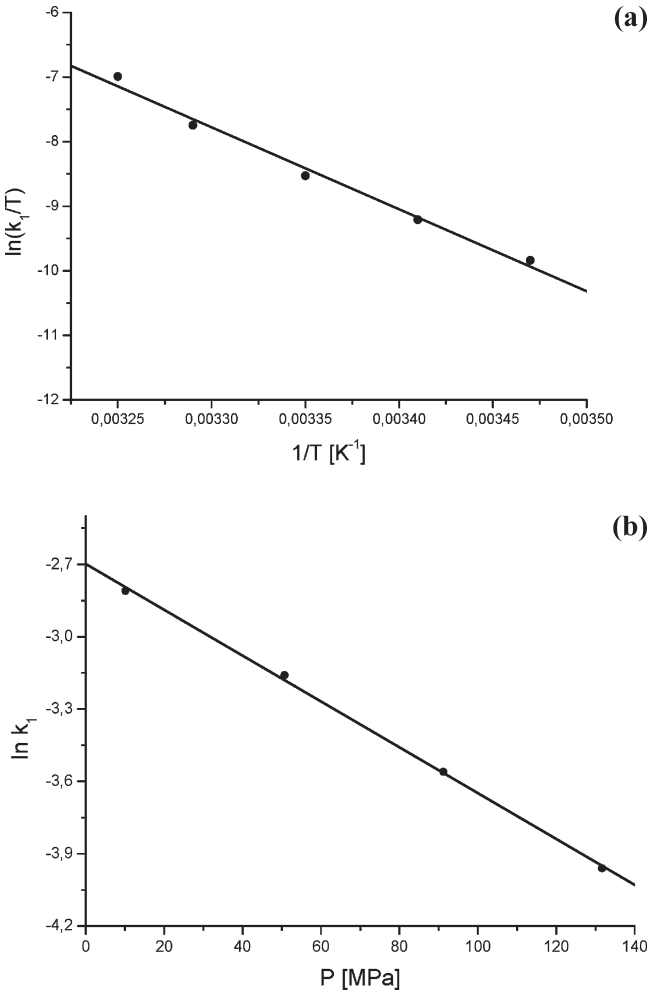

Figure 10. Temperature and pressure dependence of k_1 for the binding of NO to (TMPS)Fe^{III}(OH)(MeIm) in [emim][NTf_2]. Experimental conditions: [(TMPS)Fe^{III}(OH)(MeIm)] = 2.5×10^{-6} M, [NO] = 5 mM, λ = 434 nm.

coordinated (TMPS)Fe^{III}(OH)(MeIm) species without displacement of the hydroxy ligand by a MeIm molecule. The spin state of the iron(III) center hereby changes from pure high-spin ($S = 5/2$) to an admixed spin state ($S = 5/2, 3/2$) with a contribution of the intermediate spin ($S = 3/2$) of 69%.[42] Thus the overall spin state change on the binding of NO to (TMPS)Fe^{III}(OH)(MeIm) ($S = 5/2$, $3/2 \rightarrow S = 0$), which is smaller than for (TMPS)Fe^{III}(OH) ($S = 5/2 \rightarrow S = 0$), plays an inferior role and has no influence on the kinetics.[43]

As outlined in Table 1, pure [emim][NTf_2] clearly decreases the rate of the reaction with NO as compared to a basic aqueous solution, whereas the overall reaction mechanism seems to be unchanged. Contaminations of MeIm on the other hand extremely decelerate the binding of NO accompanied by a change in mechanism from an associative (A) to a dissociative (D) mechanism. Although Figure 4 implies that in aqueous solution

(42) The percentage of 3/2 spin admixture is estimated by the empirical equation Int% = $[(80 - \delta)/140] \times 100$ (%) where δ is the shift of β-pyrrole ^{1}H resonance, compare ref 40.

(43) In aqueous solution, spin admixture is also observed at low pH for (TMPS)$Fe^{III}(H_2O)_2$. Although the binding of NO occurs according to a dissociative (D) mechanism, (TMPS)$Fe^{III}(H_2O)_2$ reacts faster than (TMPS)Fe^{III}(OH) because of the smaller overall spin state change. See ref 23.

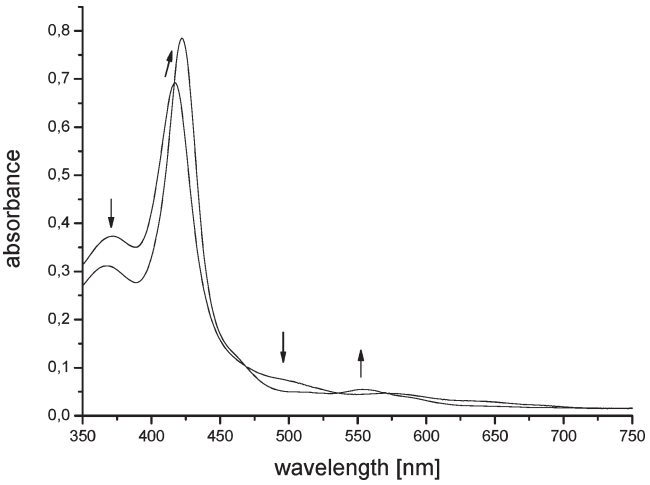

Figure 11. Spectral change accompanying the reaction of (TMPS)-Fe^{III}(OH) with NO_2^- in [emim][NTf_2]. Experimental conditions: [(TMPS)Fe^{III}(OH)] = 7.5×10^{-6} M, [NO_2^-] = 3.75×10^{-3} M, optical path length 1 cm.

(TMPS)Fe^{III}(OH)(MeIm) is only generated by the addition of a larger excess of MeIm, in the ionic liquid on the contrary even small amounts of MeIm form (TMPS)Fe^{III}(OH)(MeIm) as there are no competitive solvent effects caused by water. Therefore, the purity of alkylimidazolium based ionic liquids is of crucial importance for mechanistic investigations on sensitive systems performed in such ionic liquids.

Reaction of (TMPS)Fe^{III}(OH) with Nitrite. During our studies on the binding of NO we sometimes noticed a red shift of the Soret band to 424 nm and a characteristic fingerprint spectrum below 400 nm, which indicated the presence of nitrite impurities[44] and seemed to react with (TMPS)Fe^{III}(OH). From the literature it is known that porphyrins with negatively charged substituents at the *meso*-positions do not bind nitrite. This behavior is ascribed to an increase of electron density at the porphyrin iron center via an inductive effect of the charged substituents.[36,37] The ionic liquid appears to change this property, possibly by neutralization of the negatively charged substituents by the surrounding solvent cations. For that reason we extended our studies to the binding of nitrite to (TMPS)Fe^{III}(OH).

The addition of tetrabutylammoniumnitrite as a soluble nitrite source to a solution of (TMPS)Fe^{III}(OH) led to characteristic spectral changes which clearly differ from those observed for the formation of (TMPS)Fe^{II}(OH)(NO^+). As can be seen in Figure 11, the bands in the spectrum of (TMPS)Fe^{III}(OH) at 417, 500, and 640 nm on reaction with nitrite change to 424 and 553 nm to yield (TMPS)Fe^{III}(OH)(NO_2^-). The observed spectrum is in good agreement with the results found for another, positively charged porphyrin complex in aqueous solution.[36]

$$(\mathrm{TMPS})\mathrm{Fe^{III}(OH)} + \mathrm{NO_2^-} \underset{k_{off}}{\overset{k_{on}}{\rightleftarrows}} (\mathrm{TMPS})\mathrm{Fe^{III}(OH)(NO_2^-)} \quad (6)$$

(44) Wolak, M.; Stochel, G.; Hamza, M.; van Eldik, R. *Inorg. Chem.* **2000**, *39*, 2018–2019.

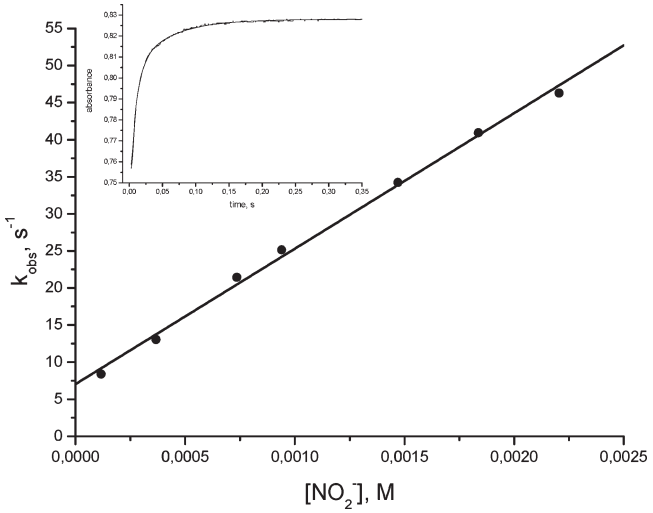

Figure 12. Concentration dependence of k_{obs} for the reaction of (TMPS)Fe^{III}(OH) with NO_2^- in [emim][NTf_2]. Experimental conditions:[(TMPS)Fe^{III}(OH)] = 7.5×10^{-6} M, λ = 424 nm, T = 25 °C. Inset: typical kinetic trace, [NO_2^-] = 3.5×10^{-4} M.

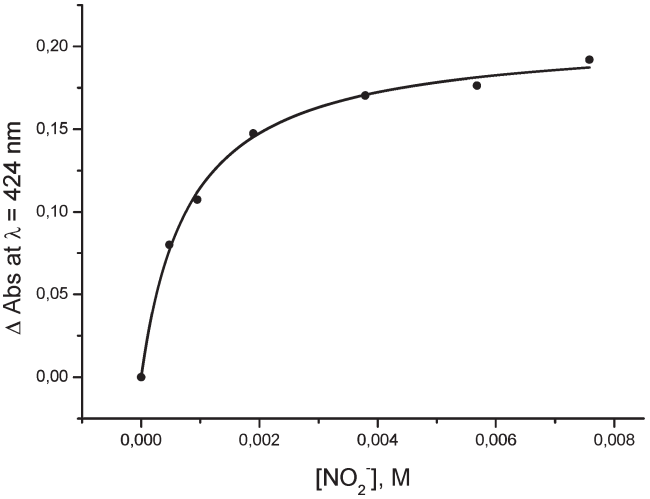

Figure 13. Change in absorbance at 424 nm for the reaction of (TMPS)Fe^{III}(OH) with NO_2^- in [emim][NTf_2]. Experimental conditions: [(TMPS)Fe^{III}(OH)] = 7.5×10^{-6} M, λ = 424 nm T = 25 °C.

Surprisingly, the reaction of (TMPS)Fe^{III}(OH) with nitrite is very fast compared to the reaction with NO. Kinetic measurements were performed under pseudo-first-order conditions up to a 300 fold excess of nitrite over (TMPS)Fe^{III}(OH). For this fast reaction the mixing process in the stopped-flow apparatus seemed to have an influence on the observed traces, and they were therefore fitted to a two-exponential function to correct for this complication. A linear plot of k_{obs} (k_{obs} is the rate constant determined from the kinetic traces following complete mixing) versus [NO_2^-] obtained at 25 °C (see Figure 12) allowed the calculation of $k_{on} = (1.82 \pm 0.05) \times 10^4$ M^{-1} s^{-1} and $k_{off} = 7.0 \pm 0.6$ s^{-1} from the slope and intercept, respectively. The overall equilibrium constant was found to be $K_{eq} = k_{on}/k_{off} = (2.6 \pm 0.3) \times 10^3$ M^{-1}. Unfortunately the viscosity of the ionic liquid, which increases with decreasing temperature and increasing pressure,[45] limits the applicability of the stopped-flow method for fast reactions. Thus, as a result of the high rate constants we were not able to determine the thermal and pressure activation parameters for this reaction. However, we assume that binding of nitrite to (TMPS)-Fe^{III}(OH) occurs according to an associative mechanism similar to the reaction with NO.

As demonstrated above, the kinetic observations indicated the presence of an equilibrium between (TMPS)-Fe^{III}(OH) and (TMPS)Fe^{III}(OH)(NO_2^-). Measurements on the thermodynamic behavior of this equilibrium as a function of temperature and pressure should enable the determination of the standard reaction parameters $\Delta H°$, $\Delta S°$ and $\Delta V°$, respectively.[46]

We first checked the kinetically determined equilibrium constant by performing a spectrometric titration for the reaction with nitrite by following the change in absorbance (ΔAbs) at 424 nm for the addition of various concentrations of nitrite to (TMPS)Fe^{III}(OH) as shown in Figure 13. K_{eq} was calculated according eq 7, where A_0 and A_∞ represent the absorbance of (TMPS)Fe^{III}(OH) and (TMPS)Fe^{III}(OH)(NO_2^-), respectively, and A_x is the absorbance at any nitrite concentration. From the data in Figure 13, K_{eq} was found to be $(1.23 \pm 0.09) \times 10^3$ M^{-1} which is in close agreement with the kinetically determined value.

$$A_x = A_0 + \frac{(A_\infty - A_0)K_{eq}[NO_2^-]}{1 + K_{eq}[NO_2^-]} \quad (7)$$

To determine the standard reaction parameters $\Delta H°$ and $\Delta S°$, the change in absorbance was followed at a 125 fold excess of nitrite ([NO_2^-] = 9.38×10^{-4} M) over (TMPS)Fe^{III}(OH) in the temperature range 15–40 °C. Figure 14 shows that the back reaction (see eq 6) is favored on increasing the temperature. K_{eq} values were calculated as a function of temperature using the calibration curve in Figure 13. A linear plot of ln K_{eq} versus $1/T$ (see Figure 14) enabled the calculation of $\Delta H° = -59 \pm 1$ kJ mol^{-1} and $\Delta S° = -141 \pm 3$ J K^{-1} mol^{-1} from the slope and intercept, respectively, according to eq 8.

$$R \ln K_{eq} = -\frac{\Delta H^o}{T} + \Delta S^o \quad (8)$$

The pressure dependence of the equilibrium constant was studied at pressures up to 150 MPa. As shown in Figure 15, increasing pressure favors the binding of nitrite and thus leads to a spectral shift of the Soret band toward 424 nm. According to eq 9, a linear fit of ln K_{eq} versus pressure obtained at 25 °C (see Figure 15) allows the calculation of $\Delta V^o = -32 \pm 1$ cm^3 mol^{-1}.

$$\ln K_{eq} = -\frac{P}{RT}\Delta V^o \quad (9)$$

In summary, Figures 14 and 15 show that increasing temperature and pressure have opposite effects on the binding of nitrite to (TMPS)Fe^{III}(OH). The temperature dependence clearly illustrates that the overall equilibrium

(45) Doldize, T. D.; Khoshtariya, D. E.; Illner, P.; van Eldik, R. *J. Phys. Chem. B* **2008**, *18*, 2112–2114.
(46) Hamza, M. S. A.; Zou, X.; Banka, R.; Brown, K. L.; van Eldik, R. *Dalton Trans.* **2005**, 782–787.

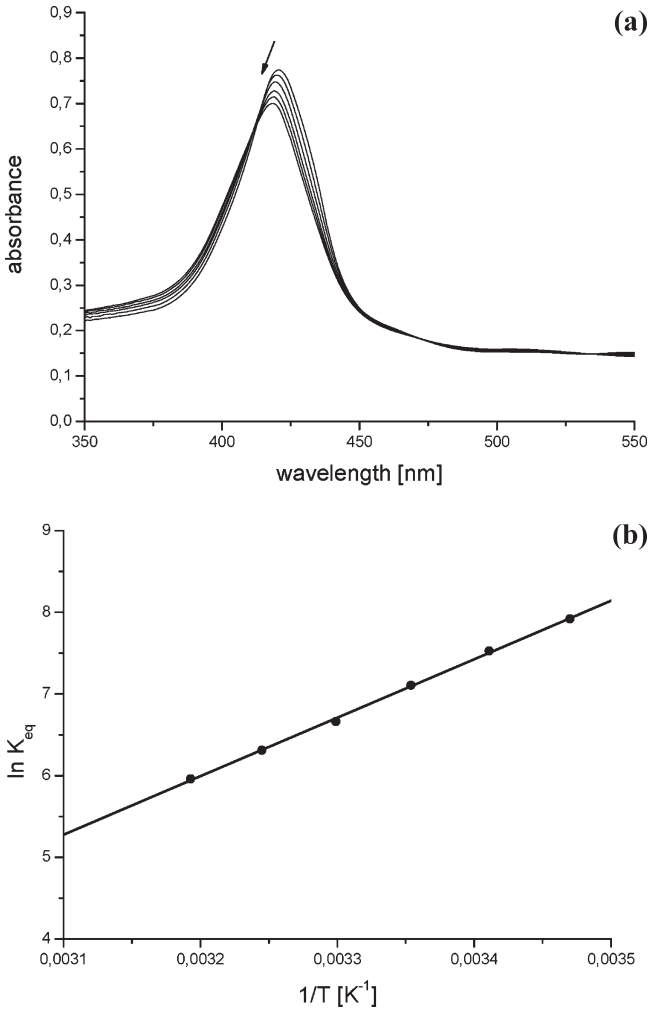

Figure 14. Temperature dependence of UV−vis spectra and Gibbs−Helmholtz plot. Experimental conditions: $[(TMPS)Fe^{III}(OH)] = 7.5 \times 10^{-6}$ M, $[NO_2^-] = 9.4 \times 10^{-4}$ M, $T = 15-40$ °C.

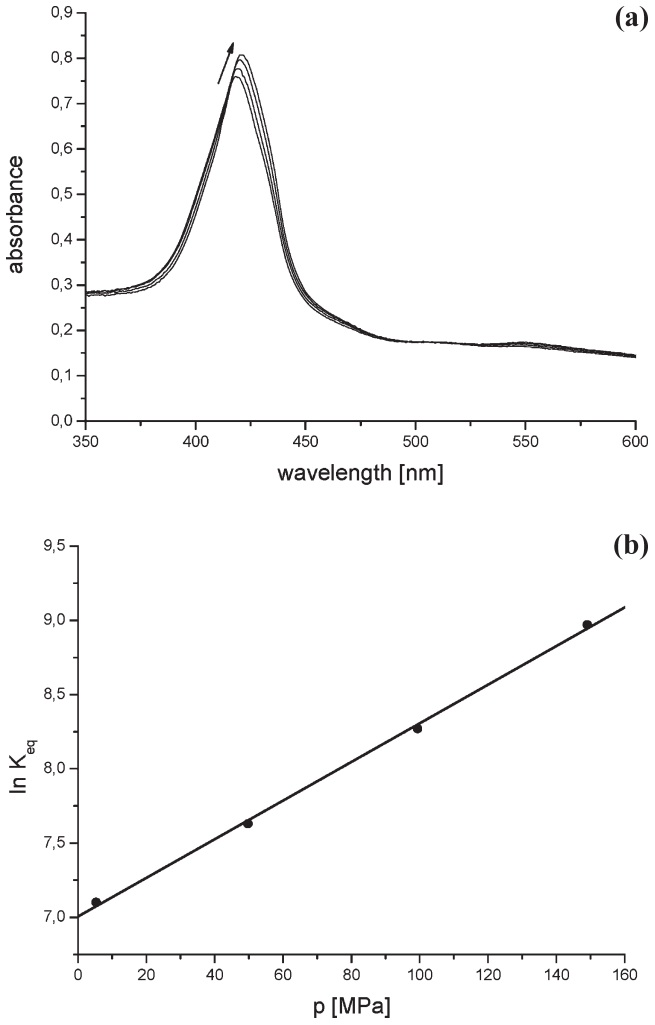

Figure 15. Pressure dependence of UV−vis spectra and plot of ln K_{eq} versus pressure. Experimental conditions: $[(TMPS)Fe^{III}(OH)] = 7.5 \times 10^{-6}$ M, $[NO_2^-] = 9.38 \times 10^{-4}$ M, $p = 5-150$ MPa, $T = 25$ °C.

(eq 6) is shifted in the backward direction on increasing the temperature, that is, according to an exothermic reaction for which $\Delta H°$ has a negative value (see Table 2). On the contrary, an increase in pressure leads to a forward shift of equilibrium (eq 6) and favors the formation of $(TMPS)Fe^{III}(OH)(NO_2^-)$. This can be explained by a significant decrease in the partial molar volume of the product on the coordination of nitrite ($\Delta V° = -32$ cm^3 mol^{-1}). The relatively large negative values of $\Delta S°$ and $\Delta V°$ can be ascribed to the coordination of nitrite and an increase in electrostriction of the solvent shell by the product species. Similar values are also reported for the binding of NO to other 5-fold coordinated iron(III) porphyrins.[47] Therefore, $\Delta V°$ is more negative than the partial molar volume of nitrite (i.e., 26 cm^3 mol^{-1}).[48] This indicates that charge concentration and intrinsic bond formation lead to a significant decrease in partial molar volume during the formation of $(TMPS)Fe^{III}(OH)(NO_2^-)$.

Table 2. Equilibrium Constants and Standard Reaction Parameters for the Binding of NO_2^- to $(TMPS)Fe^{III}(OH)$ in [emim][NTf_2]

Equilibrium Constants and Standard Reaction Parameters	
K_{eq} (kinetic at 25 °C) (M^{-1})	$(2.6 \pm 0.3) \times 10^3$
K_{eq} (thermodynamic at 25 °C) (M^{-1})	$(1.2 \pm 0.1) \times 10^3$
$\Delta H°$ (kJ mol^{-1})	-59 ± 1
$\Delta S°$ (J K^{-1} mol^{-1})	-141 ± 3
$\Delta V°$ (cm^3 mol^{-1})	-32 ± 1

Conclusions

The results obtained demonstrate clearly that a wide range of research techniques can be applied in the study of ionic liquids as done for conventional molecular solvents. For the very first time, we were able to perform high pressure stopped-flow kinetic measurements on a reaction in an ionic liquid and to confirm mechanistic conclusions based on the interpretation of thermal activation parameters. As could be seen from the reaction with nitrite, the investigation of very fast reactions unfortunately is limited by the viscosity of the ionic liquid, and therefore other research methods have to be considered. However, our results also revealed two fundamental problems. On the one hand, many reactions that are well understood in conventional solvents are performed in ionic liquids, although it is completely unclear if the catalytic

(47) Franke, A.; Hessenauer-Ilicheva, N.; Meyer, D.; Stochel, G.; Woggon, W.-D.; van Eldik, R. *J. Am. Chem. Soc.* **2006**, *128*, 13611–13624.
(48) Millero, F. J. In *Water and Aqueous Solutions: Structure, Thermodynamics and Transport Processes*; Horne, R. A. Ed.; Wiley-Interscience: London, 1972; Chapter 13.

active species react according to the same mechanism or how the ionic liquid really influences the system. The binding of nitrite to (TMPS)Fe^{III}(OH) is an example for a reaction that occurred in an ionic liquid without being observed in aqueous solution. Such unknown reactions could be very problematic and have a large influence on a system. On the other hand, trace impurities can also interact with a catalytically active species and therefore accelerate or decelerate a reaction, or even change its mechanism. As could be seen from the reaction of (TMPS)Fe^{III}(OH) with NO, the purity of the ionic liquid is of crucial importance for all investigations performed in ionic liquids, and even traces of impurities, which could be extremely difficult to detect, could have remarkable effects on the rate and mechanism of the studied reaction. Thus, many more attempts have to be undertaken to quantify and remove impurities to clarify exceptional results in ionic liquids.

Acknowledgment. The authors gratefully acknowledge financial support from the Deutsche Forschungsgemeinschaft through SPP 1191 (Ionic Liquids). We thank Katia Kreuz from the Chair of Chemical Engineering I (Reaction Engineering), University of Erlangen-Nürnberg, for performing the Karl Fischer titrations. We also thank Professor Axel Koenig and Jose Luis Sola Cervera from the Chair of Separation Science & Technology, University of Erlangen-Nürnberg, for performing the HPLC analysis of [emim][NTf_2].

Supporting Information Available: HPLC analysis of [emim][NTf_2], UV−vis, and ^{1}H NMR spectra of [(TMPS)Fe^{III}(OH)] as a function of added imidazole concentration (3 pages). This material is available free of charge via the Internet at http://pubs.acs.org.